Development of a prototype device for near real-time surface-enhanced Raman scattering monitoring of biological samples

Elodie Dumont[a]*, Charlotte De Bleye[a], Gilles Rademaker[b], Laureen Coïc[a], Julie Horne[a], Pierre-Yves Sacré[a], Olivier Peulen[b], Philippe Hubert[a], Eric Ziemons[a]

[a] University of Liege (ULiege), CIRM, VibraSanté Hub, Department of Pharmacy, Laboratory of Pharmaceutical Analytical Chemistry, CHU, B36, B-4000 Liege, Belgium.

[b] University of Liege (ULiege), Metastasis Research Laboratory, Giga Cancer, CIRM, CHU, B36, B-4000 Liege, Belgium.

[*] **Corresponding author**: E. Dumont, University of Liege (ULiege), CIRM, VibraSanté Hub, Department of Pharmacy, Laboratory of Pharmaceutical Analytical Chemistry, CHU, B36, B-4000 Liege, Belgium

Fax: +32-43.66.43.17. Phone: +32-43.66.43.24 E-mail address: elodie.dumont@uliege.be

Abstract

With the fast growth of bioanalytical surface-enhanced Raman scattering (SERS), analytical methods have had to adapt to the complex nature of biological samples. In particular, interfering species and protein adsorption onto the SERS substrates have been addressed by sample preparation steps, such as precipitation or extraction, and by smart SERS substrate functionalisation. These additional handling steps however result in irreversible sample alteration, which in turn prevents sample monitoring over time.

A new methodology, that enables near real-time, non-invasive and non-destructive SERS monitoring of biological samples, is therefore proposed. It combines solid SERS substrates, benefitting from liquid immersion resistance for extended periods of time, with an original protein filtering device and an on-field detection by means of a handheld Raman analyser. The protein removal device aims at avoiding protein surface fouling on the SERS substrate. It consists of an ultracentrifugation membrane fixed under a cell culture insert for multi-well plates. The inside of the insert is dedicated to containing biological samples. The solid SERS substrate and a simple medium, without any protein, are placed under the insert. By carefully selecting the membrane molecular weight cutoff, selective diffusion of small analytes through the device could be achieved whereas larger proteins were retained inside the insert. Non-invasive SERS spectral acquisition was then carried out through the bottom of the multi-well plate. The diffusion of a SERS probe, 2-mercaptopyridine, and of a neurotransmitter having a less intense SERS signal, serotonin, were first successfully monitored with the device. Then, the latter was applied to distinguish between subclones of cancerous cells through differences in metabolite production.

This promising methodology showed a high level of versatility, together with the capability to reduce cellular stress and contamination hazards.

Keywords: Surface-Enhanced Raman Scattering (SERS); Solid SERS substrates; Protein corona; Biological samples; Handheld Raman spectrophotometer; Near real-time monitoring.

1. Introduction

Metabolomics, which studies the low molecular weight compounds (the metabolome) produced by biological systems, is being increasingly applied to cell cultures [1-4]. The analysis of cell cultures has indeed some advantages over animal or human studies: cell cultures are for instance easier to control, present fewer confounding factors and fewer individual variations, are cheaper and raise fewer ethical issues [1-3]. Cell metabolomics can be subdivided in metabolic fingerprinting and footprinting [5]. The former concerns the measurement of the endometabolome, i.e. intracellular metabolites, while the latter is related to the exometabolome which consists in metabolites secreted or excreted in, or consumed from the extracellular medium [3,5]. Despite complementing one another, metabolic footprinting can be more convenient than fingerprinting as it does not require cell lysis and consequently enables monitoring of the same sample over time, which is particularly valuable for cells available in a limited amount [3]. By their nature, several applications, such as the monitoring of cellular responses to external stimuli, cellular differentiation, or bioprocesses, also require non-destructive real-time or near real-time monitoring [6-8]. Moreover, metabolic footprinting raises fewer technical issues since it does not call for fast cell metabolism quenching nor for intracellular metabolites extraction [5]. Because cells constantly exchange metabolites with the environment, probing the exometabolome can give some insight into the metabolic activity of the cells and their response to various stimuli [3,5,9]. Extracellular culture medium analyses have therefore been conducted notably in order to study the impact of drugs, chemicals or infections on cells [6,9-14], to discriminate cancer from healthy cells [15,16], to follow cellular differentiation [7] or to optimise biotechnological processes [8,17,18]. However, these applications often rely on invasive sampling of the culture medium, which is subsequently analysed with at-line analytical techniques such as chromatography coupled to mass spectrometry or nuclear magnetic resonance [7-18]. This runs the risk of contaminating the sample or making the cells stressed.

Surface-enhanced Raman scattering (SERS) has been steadily expanding over the last few years owing to its multiple advantages [19-24]. One of the fastest growing field, bioanalysis, has in particular benefited from the detection sensitivity and specificity, as well as from the lack of spectral interference from water and air of this analytical technique [19,20]. Bioanalytical SERS encompasses a wide variety of applications, ranging from small metabolites or protein biomarkers quantification to whole cell sensing and sorting [19,20]. Extracellular metabolites

determination notably received attention as it can assist in disease diagnosis and cellular differentiation [25-29]. However, these applications share a common feature, intricate biological matrices, that often contain proteins [19,20]. On one hand, the presence of such amounts of interfering species can hamper analyte detection by competing for the SERS substrate surface. On the other hand, the adsorption of proteins onto nanomaterial surfaces, forming a so-called protein corona, is a well-established phenomenon [30]. This protein corona further competes with analytes for adsorption onto SERS substrates. It can moreover sharply decrease or even suppress the SERS signal enhancement by stabilising suspensions of nanoparticles (NPs), thereby hindering hot-spot formation [31,32].

To deal with these bioanalytical issues in SERS, diverse strategies have been implemented. They mainly rely on additional sample handling and preparation steps, such as protein precipitation [33,34], sample extraction [35] or SERS substrate smart functionalisation with antibodies, aptamers or molecularly imprinted polymers for instance [36-38]. More simply, NPs can be pre-aggregated to get around the protein corona stabilisation problem [31,39]. In all these studies, the sample is consequently irremediably modified, hence making sample monitoring over extended time span impossible. Regarding cellular metabolites determination, SERS experiments are still currently primarily carried out on cell conditioned media, cell culture supernatants or cell lysates, that are put in contact with the SERS substrate after sampling [25-28,40,41]. These supplementary sampling steps can be a source of cell culture contamination, cellular stress and/or sample destruction, though.

The use of solid SERS substrates could be a solution to the destructivity problem in bioanalytical SERS, since these substrates already include preformed hot-spots and can remain intact when they are immersed in the sample [42]. Solid SERS substrates can be categorised as disordered (bottom-up) and ordered (top-down) according to the level of nanostructure organisation [43]. While the former can be synthesised easily and at low cost, for example starting from suspensions of NPs, the latter require more sophisticated, thus expensive, preparation technologies to achieve a higher degree of structural precision [42-44]. Yet, the surface of these solid SERS substrates is still prone to protein fouling and must consequently be protected. To that end, two options can be considered: either functionalising the substrate surface with anti-fouling coatings or removing proteins from the analysed medium [44]. The former alternative suffers from the difficulty to find biocompatible anti-fouling coatings that are still able to attract the analyte of interest near the substrate surface and that do not interfere

with its SERS detection [44]. This often necessitates combining the anti-fouling coating with a smart surface modifier [44]. Moreover, surface functionalisation is not a straightforward process. It requires multiparametric optimisation to be properly mastered and regularly rests on complicated spectral interpretation due to the presence of an additional interface between the metal surface and the analyte [44,45].

This is why, in this work, an original device preventing protein adsorption onto the solid SERS substrate was designed. This device derived from the use of ultracentrifugation membranes as effective protein filtration element between 2 compartments: the upper one containing the biological sample and the bottom one holding a solid SERS substrate and a clean collection medium like phosphate buffer. The SERS substrate was simply prepared by immobilising gold nanoparticles (AuNPs) onto a glass support by means of electrostatic interactions. Combined with handheld Raman detection, whose acquisition parameters were optimised through the design of experiments (DoE) approach, this device enabled near real-time non-invasive SERS monitoring of biological samples. As a proof-of-concept, the discrimination between highly and weakly metastatic pancreatic ductal adenocarcinoma cells could be established based on differential production rates of cellular metabolites. With the recent outbreak of SERS spectral databases of metabolites [46], the developed device seems promising and could pave the way to a new kind of metabolic footprinting SERS analysis.

2. Material and methods

2.1 *Chemicals and reagents*

Gold(III) chloride hydrate (99.995% trace metals basis), poly-L-lysine hydrobromide (molecular weight 70,000-150,000, lyophilized powder, γ-irradiated, BioXtra, suitable for cell culture), 2-mercaptopyridine (2-MP, 99%) and Dulbecco's modified Eagle's medium (DMEM) were acquired from Sigma-Aldrich (St. Louis, MO, USA). Merck (Darmstadt, Germany) was the supplier of nitric acid (65%, for analysis), sodium chloride (for analysis) and di-sodium hydrogen phosphate (for analysis). Potassium dihydrogen phosphate (Reag. Ph. Eur.) and hydrochloric acid (37%, for analysis) were purchased from VWR Chemicals (Leuven, Belgium). Acros Organics (Geel, Belgium) was the supplier of trisodium citrate (anhydrous, 98%). Serotonin hydrochloride (5-HT, >97%) was acquired from TCI Europe (Zwijndrecht, Belgium). All chemicals were used as received. Ultrapure water with a resistivity of 18.2 MΩcm, was used for the preparation of aqueous solutions and was generated from a Milli-Q device (Millipore, Bellirica, MA, USA). Phosphate buffered saline (PBS) and RPMI-1640 without glutamine were furnished by Lonza (Verviers, Belgium). Gibco by Life Technologies (Carlsbad, CA, USA) was the supplier of heat-inactivated horse serum (HS) and foetal bovine serum (FBS).

2.2 *SERS substrate preparation*

Borosilicate glass coverslips (18 mm diameter, 0.16 mm thickness (No 1.5), VWR) were first decontaminated with aqua-regia (65% HNO_3 and 37% HCl, in a 1:3 (v/v) proportion). They were afterwards covered with a 0.1 g/L aqueous poly-L-lysine hydrobromide solution and placed in an incubator at 40°C and 75% relative humidity during 3 h. After this step, the coverslips were rinsed with ultra-pure water and air dried. Then, 510 µL of citrate reduced AuNPs, previously synthesised according to the Lee & Meisel protocol [47], were dropped on each coverslip to form a large drop covering the whole coverslip surface. These drops were kept by capillary forces on the coverslips and were left undisturbed and away from light during two days. This step allowed the AuNPs to settle and adhere to the poly-L-lysine coated coverslip. Finally, the AuNPs-coated coverslips (Au-coverslips) were rinsed with ultra-pure water and air dried.

2.3 *Protein removal device*

The developed protein removal device is described in Fig. 1. Hanging cell culture inserts for 12-well culture plates (Millicel®, Merck, Darmstadt, Germany) were the basis of the protein removal device. The polyethylene terephthalate membrane of these inserts had a 12 mm diameter and a 0.4 µm pore size. Polyethersulfone (PES) and Hydrosart® ultracentrifugation membranes were purchased from Sartorius (Göttingen, Germany) and had a molecular weight cutoff (MWCO) of 1 kDa and 5 kDa, respectively. Discs of 16 mm diameter were cut out from these ultracentrifugation membranes with the help of a sharp metal cylinder. This diameter matched the diameter of the bottom of the cell culture inserts. The ultracentrifugation membrane disks were then glued (Loctite® Super glue-3, ethyl 2-cyanoacrylate) under the bottom part of the cell culture inserts, with the effective centrifugation side facing upwards toward the cell culture insert. The obtained device was then placed in a 12-well plastic cell culture plate (Greiner Bio-One, Kremsmünster, Austria) that already contained an Au-coverslip. When the bottom of the 12-well cell culture plate was interfering in the SERS detection, it was removed by heat. To that end, a sharp metal cylinder of 10 mm diameter was heated with the flame of a Bunsen burner and was then quickly used to meld the plastic of the culture plate. The resulting circular hole was sealed by gluing an Au-coverslip on top of it, with its SERS active side facing upwards.

2.4 *Equipment*

The TruScan™ RM handheld Raman analyser, embedding the TruTools™ package (Thermo Fisher Scientific, Waltham, MA, USA), was used to conduct non-invasive measurements through the bottom of 12-well cell culture plates. This handheld spectrophotometer was equipped with a 785 nm laser of 250 mW and covered the 250-2875 cm^{-1} spectral range. Three spectra, each one consisting of 4 repetitions of 10 s, were taken at different places on each sample (the optimisation of these acquisition parameters is described in Supplementary Material, part 1 “Optimisation of the TruScan™ acquisition parameters”). For spectral comparison and confirmation analysis, a LabRAM HR Evolution Raman microscope (Horiba Jobin-Yvon, Lyon, France) was employed. It was equipped with a 785 nm laser (50 mW on the sample), a 50x LWD objective and a two-dimensional EMCCD detector (1600 x 200 pixels sensor). A 300 gr/mm grating was selected and the spectra were acquired either in the 350-1750

187 cm^{-1} or in the 100-3200 cm^{-1} (for cellular applications) spectral range. Three spectra were
188 collected at the same location on each sample with an acquisition time of 7 s.

189 ## 2.5 *Diffusion tests*

190 The diffusion process of analytes from the cell culture insert to the collection medium was
191 checked with 2-MP first since it has an intense and characteristic SERS signature. The
192 characteristic bands of 2-MP can thus easily be tracked. Non-invasive monitoring and invasive
193 sampling from the collection medium were carried out to compare the results obtained by these
194 two analysis configurations. Then, the diffusion of analytes with weaker SERS activities was
195 considered. A monoamine neurotransmitter, serotonin (5-HT) was selected given its
196 physiological importance in central as well as peripheral functions, its involvement in numerous
197 pathologies and the high affinity of its indole amine for gold surfaces [48-50].

198 The culture medium used for the development stage of the protein removal device was
199 composed of RPMI-1640 supplemented with 10% HS and 5% FBS.

200 For 2-MP, an Hydrosart® membrane was used as filter. The collection medium consisted of
201 1.25 mL pure RPMI-1640. 1.25 mL of complete culture medium (with HS and FBS, as defined
202 above) was placed in the insert. 132 µL of 200 µM 2-MP solution prepared in RPMI-1640 were
203 added in the insert, leading to a final 2-MP concentration of 10 µM. The 12-well plate was left
204 in a cell culture incubator (37°C, 5% CO_2) throughout the course of the diffusion test. Regarding
205 invasive monitoring, samplings of 55 µL collection medium were realised over time. 50 µL of
206 these samples were mixed with 400 µL AuNPs and 400 µL of the resulting mixture were
207 immediately analysed under the Raman microscope in a 96-well plate.

208 For 5-HT, a PES membrane was used as filter. 1.25 mL of PBS was poured over an Au-
209 coverslip as collection medium and 1.25 mL of culture medium was placed in the insert. 132
210 µL of a 500 ppm (2.35 mM) 5-HT solution prepared in RPMI-1640 were added in the insert,
211 leading to a final 5-HT concentration of 25 ppm (117.5 µM). For the blank samples, 132 µL of
212 RPMI-1640 were added instead of 5-HT. The 12-well plates were left in a cell culture incubator
213 (37°C, 5% CO_2) throughout the course of the diffusion test.

214 The experimental pancreatic ductal adenocarcinoma liver metastases model developed by
215 Rademaker *et al.* [51] was selected to assess the protein removal device in a cellular
216 environment. It consisted of 2 subclones of Panc-1 cells: high metastatic cells (HM) and low

metastatic cells (LM) obtained after 3 rounds of *in vivo* selection of liver-tropic (for HM) or spleen-remaining (for LM) Panc-1 cells injected in the spleen of immunodeficient mice [51]. The cells were cultured in DMEM supplemented with 10% FBS, 1% penicillin streptomycin and 0.4% amphotericin B and were incubated at 37°C in an atmosphere containing 5% CO_2. A first set of experiments was carried out on conditioned HM and LM cell culture media. PES ultracentrifugation membranes were used as filters. 1.25 mL of PBS was poured over an Au-coverslip as collection medium and 1.25 mL of conditioned culture medium was placed in the insert. A blank sample of pure culture medium was also prepared. The 12-well plates were left in a cell culture incubator (37°C, 5% CO_2) throughout the course of the experiment. Regarding experiments conducted on cells, the same was done, except that 1.25 mL culture medium containing living HM or LM cells was placed in the inserts. HM and LM cells were seeded at 3 different densities: 5, 10 and 20 $x10^4$ (thereafter abbreviated HM or LM5, 10 and 20, n = 1). Again, a blank sample consisting of pure culture medium was also prepared. For orthogonal confirmatory analyses on the LabRAM Raman microscope, 400 µL of AuNPs were pre-aggregated with 90 µL of concentrated PBS (PBSx10; 1.44 g/L KH_2PO_4, 7.95 g/L Na_2HPO_4 and 90 g/L NaCl). Then, 44 µL of collection medium, sampled in sterile conditions at several time points, were added to the aggregated AuNPs [31]. 400 µL of the resulting mixture were placed in a 96-well plate and immediately analysed.

2.6 *Data analysis*

The SERS spectra were analysed with Matlab R2018a (The Mathworks, Natick, MA, USA) and the PLS_Toolbox 8.6.2 (Eigenvector Research, Inc., Wenatchee, WA, USA). For TruScan™ data, the spectra resulting from 3 measurement repetitions were averaged. The baseline of all spectra was corrected with an automatic Whittaker filter (the λ and p parameters values were 10^5 and 0.001, respectively) and they were then smoothed with the Savitzky-Golay algorithm (width of 13, polynomial order of 2 and no derivative).

Principal component analysis (PCA) on diffusion experiments were conducted on the TruScan™ pre-processed and mean centred data. The spectral range was restricted from 437.2 to 1748.9 cm^{-1}, except for the cellular applications of the device (range between 250 and 2250.7 cm^{-1}). When present, the most intense bands of polystyrene (975 to 1053 cm^{-1}) were also removed from the spectrum.

3. Results and discussion

3.1 *Development of the protein removal device*

Since the SERS signal not only depends on the SERS substrate but also on the instrument used to make the measurements [52], the SERS substrate repeatability and stability and the influence of the handheld Raman analyser acquisition parameters were studied in a first stage. Results related to this section are described in Supplementary Material (part 2, "Assessment of the SERS substrate"). In brief, the average RSD of the substrate was around 20% and its spectral signature quickly evolved over time, possibly due to oxidation of surface adsorbed citrate [53]. In view of this, spectra acquired on this SERS substrate during future monitoring will automatically comprise a variable component linked to the substrate itself. Care must therefore be taken to make a distinction between signal variation related to the substrate and to the sample. Chemometric tools could provide valuable assistance in that respect, as will be demonstrated in the next sections of this paper.

A device was then developed to remove the proteins from the analysed medium. It consisted of a cell culture insert, in which can be put the sample to be studied (cells with their culture medium for example), placed in a well of a 12-well plate. Under the insert, a collection medium was poured, which was a simple matrix that does not contain any proteins, such as PBS or RPMI. The element of the device responsible for protein retention inside the insert was an ultracentrifugation membrane glued below the bottom part of the insert. By appropriately choosing the MWCO and material of this membrane, selective diffusion of small analytes can be attained. Indeed, most of the proteins forming the protein corona are heavier than 20 kDa [54]. This device can be used in combination with solid SERS substrates, placed at the bottom of the well, for non-invasive analyte monitoring. In this configuration, SERS spectra were acquired through the bottom of the 12-well plate thanks to a handheld Raman spectrophotometer (Fig. 1a). Moreover, invasive sampling can still be conducted from the culture and collection media with this device (Fig. 1b), in order to conduct confirmation testing for instance. The samples collected can then be mixed with suspensions of NPs or solid SERS substrates, or they can even be analysed with another analytical technique.

3.1.1 Assessment of the protein removal performances

The ability of the device to retain the proteins inside the cell culture insert was inspected by means of SERS. After 24 h incubation at 37°C, the collection medium (RPMI) and the culture medium (CM) inside the insert were sampled and analysed by mixing them with an equal volume of AuNPs. For comparison, pure RPMI was also analysed in the same way. Unsurprisingly, the CM sample failed to aggregate AuNPs due to the protein corona, which translated into the absence of SERS signal (Fig. 2, green curve). Conversely, both pure RPMI and the RPMI used as collection medium were able to trigger AuNPs aggregation, and SERS responses could be noticed for these samples (Fig. 2, blue and orange curves, respectively). The aggregation of AuNPs can be visualised on the pictures in Fig. 2 by the purple colour taken by the mixture of RPMI and AuNPs, whereas the reddish colour of the CM-AuNPs mixture is an indicator of the absence of AuNPs aggregation. Besides, bubbles were only obtained when mixing the CM with AuNPs (no bubbles in the RPMI-AuNPs nor in the collection medium-AuNPs mixtures). These bubbles are owing to the fact that proteins have surfactant properties [55]. From these experiments, it was deduced that proteins forming a corona around AuNPs were not found in the collection medium and were held back inside the cell culture insert.

3.1.2 2-Mercaptopyridine diffusion test

A first analyte having an intense SERS response, 2-MP, was selected to assess the diffusion process from the cell culture insert to the collection medium. Both non-invasive monitoring (Fig. 3a and b) and invasive sampling (Fig. 3c and d) were carried out. In both analysis methods, the specific 2-MP signature quickly appeared in the SERS spectra, demonstrating the effective migration of 2-MP through the membranes of the filter device. The intense Raman background of polystyrene, coming from the bottom of the 12-well plate, did not interfere with 2-MP non-invasive detection (Fig. 3a). 2-MP bands could nonetheless be detected faster in the spectra taken with the TruScan™ from underneath the culture plate (30 min versus 90 min for the invasive sampling). The kinetics of 2-MP detection were also different between the 2 kinds of analyses. The increase in 2-MP area followed a logarithmic trend for non-invasive Au-coverslip detection (Fig. 3b) while the trend was more linear for the samples collected and analysed with suspensions of AuNPs (Fig. 3d). These observations could be explained as follows. First, 2-MP has a high affinity for gold surfaces since it can covalently bind onto them [45]. When an Au-coverslip is placed below the filter device, it could act as a concentrator, ergo accelerating 2-MP detection compared to invasive samplings of the collection medium. Second, since the Au-

coverslip is permanently present in the collection medium, its surface will rapidly become saturated with the analyte (hence the logarithmic trend). This phenomenon is also reinforced by the lower surface area available for analyte binding when AuNPs are fixed onto a substrate in comparison with AuNPs in suspension. The "available AuNPs surface to 2-MP" ratio was besides larger in the invasive configuration thanks to the limited amounts of samples (50 µL) added to large volumes of AuNPs (400 µL).

3.1.3 Serotonin diffusion test

Then, the diffusion of serotonin (5-HT), which has a weaker SERS response than 2-MP, was investigated in order to demonstrate the potential of the device for weak SERS responders sensing. Indeed, most biologically relevant molecules have low to medium SERS responses.

A cleaner collection medium, PBS, was chosen instead of RPMI to maximise the chances of 5-HT detection. As it can be observed in Fig. S12, the weak SERS response of 5-HT, combined with the high polystyrene background coming from the bottom of the 12-well plate, made the visualisation of 5-HT bands in the spectra impossible. Bands decreasing with the incubation time were related to the Au-coverslip (as mentioned in Supplementary Material).

Resort to a multivariate data analysis technique, principal component analysis (PCA), was therefore contemplated. Among the principal components employed to construct a PCA on the data, a clear trend explaining the effect of time was noticed for the first and second principal components (PC1 and PC2, Fig. 4a). The first PC explained 95.82% of the spectral variance with a corresponding loading related to Au-coverslip signature change over time. Conversely, although PC2 only explained 1.18% of the spectral variance, the bands found in its loading were linked to 5-HT, as highlighted in Fig. 4b. These bands were located at 457, 753, 816, 1213, 1346, 1424 and 1512 cm^{-1}.

In order to improve 5-HT detection sensitivity, it was then imagined to remove the plastic bottom of the 12-well plate by melting it and to seal the subsequent hole with an Au-coverslip. This would result in the suppression of the intense polystyrene Raman background. After this additional preparation step, the diffusion of 5-HT was monitored as previously. This time, it was nevertheless possible to distinguish some weak 5-HT features appearing in the SERS spectrum with time, as flagged in Fig. S13. A PCA was once again executed on the data and a clear trend explaining the effect of time could be observed on PC1 (Fig. 5a). 5-HT characteristic

bands were found in the negative part of the PC1 loading while bands related to Au-coverslip changes were found in its positive part. The inverse of this loading was calculated and is plotted in Fig. 5b for a more convenient comparison with the reference spectrum of 5-HT (5-HT related bands appearing as positive bands).

Blank diffusion tests were also conducted with normal and bottom-removed plates to further prove that the time-related trend could actually be attributed to the diffusion of 5-HT and that this trend was not solely due to Au-coverslip modifications. PCA were constructed on the data and, in both cases, a distinct tendency that was connected to the time was noticed on the PC1. But, unlike previous diffusion tests on 5-HT samples, the PC loadings only included Au-coverslip bands (Figs. S14-S17).

Finally, the diffusion of 5-HT was investigated with a device lacking the ultracentrifugation membrane element. No tendency could be revealed by PCA, which proved the usefulness of the ultracentrifugation membrane to prevent protein fouling on the Au-coverslip surface. Even if SERS signals could still be obtained due to the presence of naturally occurring hot-spots, these signals were very weak and were mainly due to the proteins adsorbed onto the SERS substrate.

To summarise, the results obtained during this proof-of-concept study demonstrated the usefulness and the efficiency of the filter device for protein fouling prevention. It was also evidenced that the analysis configuration could be adapted to analytes that do not possess intense SERS signatures.

3.2 *Cellular application of the protein removal device*

The last step was dedicated to a cellular application of the new device, resting on previously optimised analysis conditions (acquisition parameters, Au-coverslips from the same batch and used within 2 days after preparation). A cellular model of liver metastases in pancreatic ductal adenocarcinoma was selected for this purpose [51]. This model comprises 2 subclones of Panc-1 cells: high metastatic cells (HM) and cells with a low metastatic potential (LM). While the former have been shown to have a more oxidative metabolism with increased oxidative phosphorylation and high oxygen consumption rates, the latter are more glycolytic [51]. This results in divergences in the production of the main metabolites between these subclones leading, for instance, to significant differences in the culture medium pH in contact with the

cells (Fig. S18). Indeed, through glycolysis, LM cells produce and release more acidic metabolites than HM ones, such as lactate, that contribute to the acidification of their extracellular environment. In this context, it was assessed whether the previously developed device could distinguish LM from HM cells on the basis of their difference in metabolism.

3.2.1 Distinction between conditioned cell culture media

To begin with, experiments were conducted on culture media that had been put in contact with the cells for a few days before being collected (conditioned media). This prevented introducing additional variability related to the culture medium compositional changes with time. LM and HM conditioned media were put inside the cell culture inserts, and a third insert was filled with pure culture medium (CM) as a blank sample. The diffusion process was followed with the TruScan™ through the bottom of normal (non-melted) 12-well plates during 3 days.

For all 3 samples, a striking observation was made: during the first day, the SERS signal quickly changed. This was mainly attributed to the alteration of the Au-coverslip SERS signature, as previously stated in 3.1, but analytes diffusion could also contribute to this spectral modification. Indeed, as observed in Fig. 3, it seemed that concentration equilibration on either side of the membrane filter took around one day.

This phenomenon was clearly viewed when a PCA was done on the data, with points linked to the first day of experiment segregated from the others on PC1 (Fig. 6). As indicated on Fig. 6a, a tendency that explained the effect of time was noticed on PC1 and PC2. Interestingly, after the transitory variable phase, discrimination between CM, HM and LM samples occurred on PC3 (Fig. 6b). Especially, separation of CM from HM and LM samples was rather pronounced. While PC1 and PC2 loadings included numerous bands related to the Au-coverslip evolution, PC3 contained distinct bands (Fig. S19). Fig. 7 displays the SERS spectra of CM, HM and LM samples obtained after 48h of diffusion. Despite the fact that plastic and Au-coverslip signatures account for most part of the spectra, a few spectral regions could be assigned to the sample composition, in line with PC3 displayed in Fig. S19. Taken together, these observations could support the fact that the protein removal device is able to discriminate between different culture medium compositions and that this segregation is not due to Au-coverslip signal variations. While segregation by visual inspection of the spectra was rather complex due to few weak spectral bands linked to the sample, PCA was able to handle this spectral complexity.

Orthogonal confirmatory SERS experiments were also carried out on samples taken from the collection medium under the insert at several time points (Supplementary Material, part 4.1, "Distinction between conditioned cell culture media"). These experiments confirmed the results obtained with the TruScan™.

3.2.2 Distinction between subclones

The distinction between pure culture medium (blank sample), HM and LM cells seeded in the device at 3 densities (5, 10 and 20 x10^4 cells) was then evaluated, both with the handheld Raman spectrophotometer and with the Raman confocal microscope (microscope results displayed in Supplementary Material, part 4.2, "Distinction between subclones").

Unsurprisingly, spectral changes related to the Au-coverslip surface alteration were noted during handheld Raman analyses, even if analysis only started after 16 h incubation.

It was then evaluated whether HM and LM samples could be discriminated, and whether any cell density-related tendency could be established in function of the incubation time. Compositional variations are indeed expected in the culture medium as cells will progressively produce and release metabolites. By diffusing through the membrane filter, this metabolites production will have repercussions for the collection medium content. HM and LM samples did not entirely evolve in the same way over time but could be roughly differentiated by PCA from each other and from the blank sample at any incubation time (Fig. 8). On one hand, a cell density-related pattern emerged on PC1 for HM samples during the first 2 days (Fig. 8a to c). This pattern slightly vanished after 3 days (Fig. 8d). On the other hand, an obvious trend was noticed on PC2 for LM samples, which accentuated until 24 h incubation time (Fig. 8a and b). This relationship with LM cell density then became less pronounced (Fig. 8c and d). Improving then deteriorating tendencies could be linked to the establishment of a diffusion equilibrium, followed in a second step by SERS substrate surface saturation. As LM samples evolved quicker than HM samples, it could be hypothesised that a higher amount of metabolites would be released by these cells, causing accelerated substrate saturation (results supported by Raman microscope analyses, in Supplementary Material, part 4.2, "Distinction between subclones"). Because of the high polystyrene background, identifying any band explaining these observations turned out to be arduous. SERS substrate saturation by metabolites is likely to occur when experiments are conducted over extended periods of time. This saturation phenomenon must therefore be kept in mind since it can affect the results of near real-time

SERS measurements. In order to ensure reliable results, it would be recommended to limit the duration of experiments to the time SERS substrate saturation is firstly observed.

4. Conclusion

In conclusion, a solid SERS substrate, whose preparation is rather straightforward, was successfully incorporated into a non-invasive analysis device that enables near real-time monitoring of biological samples. As a proof-of-concept, the diffusion of 2-MP and 5-HT was followed and the difference between high and low metastatic cells could be told.

This device rested upon the use of ultracentrifugation membranes as protein retention element, preventing protein corona formation onto the SERS substrate. On one hand, one of the leading strengths of the device is its versatility at several levels. Firstly, the ultracentrifugation membrane material and its MWCO can be tailored to the analyte. Secondly, the use of different kinds of solid SERS substrates, differing by their metal nature or their preparation method, could be considered. These substrates could furthermore be functionalised to specifically attract molecules lacking native affinity for the substrate surface. Thirdly, the device still enables running orthogonal confirmatory analyses in parallel with the non-invasive monitoring, since samples can be taken from the collection medium. Fourthly, as an alternative to handheld spectrophotometer detection, the solid SERS substrate in the system could be mapped under an inverted Raman microscope in order to collect more precise spatial distribution information. Lastly, the device can be adapted by removing the polystyrene bottom of the multi-well plate. By lowering the spectral background, this can favour the detection of weakly SERS responding analytes. On the other hand, the analysis protocol developed herein can minimise cellular stress and contamination issues, since it bypasses invasive sampling steps.

Finally, this proof-of-concept study underlined the promising character of the protein removal device, which could be used for near real-time SERS metabolomic footprinting analyses.

Acknowledgements

The National Fund for Scientific Research, F.R.S.-FNRS is gratefully acknowledged for the Aspirant funding granted to E. Dumont (1.A030.17F – FC6921). This work was also supported by the Fonds Léon Fredericq Foundation, Liege, Belgium (Operating grant 2019-2020). The European funds of regional development (FEDER) and the Walloon Region program "Walloon-2020.EU" are also thanked for the funding of L. Coïc.

Appendix A. Supplementary material

Supplementary data associated with this article can be found in the online version.

References

[1] M. Cuperlovic-Culf, D.A. Barnett, A.S. Culf, I. Chute, Cell culture metabolomics: applications and future directions, Drug Discov. Today 15 (2010) 610-621. https://doi.org/10.1016/j.drudis.2010.06.012

[2] A. Zhang, H. Sun, H. Xu, S. Qiu, X. Wang, Cell metabolomics, OMICS 17 (2013) 495-501. https://doi.org/10.1089/omi.2012.0090

[3] Z. Leon, J.C. Garcia-Canaveras, M.T. Donato, A. Lahoz, Mammalian cell metabolomics: Experimental design and sample preparation, Electrophoresis 34 (2013) 2762-2775. https://doi.org/10.1002/elps.201200605

[4] S. Kostidis, R.D. Addie, H. Morreau, O.A. Mayboroda, M. Giera, Quantitative NMR analysis of intra- and extracellular metabolism of mammalian cells : A tutorial, Anal. Chim. Acta 980 (2017) 1-24. https://doi.org/10.1016/j.aca.2017.05.011

[5] D.B. Kell, M. Brown, H.M. Davey, W.B. Dunn, I. Spasic, S.G. Oliver, Metabolic footprinting and systems biology : The medium is the message, Nat. Rev. Microbiol. 3 (2005) 557-565. https://doi.org/10.1038/nrmicro1177

[6] C.C. Marasco, J.R. Enders, K.T. Seale, J.A. McLean, J.P. Wikswo, Real-time cellular exometabolome analysis with a microfluidic-mass spectrometry plaform, PLoS One 10(2) (2015) e0117685. https://doi.org/10.1371/journal.pone.0117685

[7] A. Surrati, R. Linforth, I.D. Fisk, V. Sottile, D.-H. Kim, Non-destructive characterisation of mesenchymal stem cell differentiation using LC-MS-based metabolite footprinting, Analyst 141 (2016) 3776-3787. https://doi.org/10.1039/c6an00170j

[8] Z. Sun, Q. Ji, A.R. Evans, M.J. Lewis, J. Mo, P. Hu, High-throughput LC-MS quantitation of cell culture metabolites, Biologicals 61 (2019) 44-51. https://doi.org/10.1016/j.biologicals.2019.07.003

[9] A.M. Araujo, N. Moreira, A.R. Lima, M. de Lourdes Bastos, F. Carvalho, M. Carvalho, P. Guedes de Pinho, Analysis of extracellular metabolome by HS-SPME/GC–MS: Optimization and application in a pilot study to evaluate galactosamine-induced hepatotoxicity, Toxicol. Lett. 295 (2018) 22-31. https://doi.org/10.1016/j.toxlet.2018.05.028

[10] N.C. Kleinstreuer, A.M. Smith, P.R. West, K.R. Conard, B.R. Fontaine, A.M. Weir-Hauptman, J.A. Palmer, T.B. Knudsen, D.J. Dix, E.L.R. Donley, G.G. Cezar, Identifying developmental toxicity pathways for a subset of ToxCast chemicals using human embryonic stem cells and metabolomics, Toxicol. Appl. Pharmacol. 257 (2011) 111-121. https://doi.org/10.1016/j.taap.2011.08.025

[11] G. Pagla, S. Hrafnsdottir, M. Magnusdottir, R.M.T. Fleming, S. Thorlacius, B. Palsson, I. Thiele, Monitoring metabolites consumption and secretion in cultured cells using ultra-performance liquid chromatography quadrupole–time of flight mass spectrometry (UPLC-Q-ToF-MS), Anal. Bioanal. Chem. 402 (2012) 1183-1198. https://doi.org/10.1007/s00216-011-5556-4

[12] H.M. Elsheikha, M. Alkurashi, K. Kong, X.-Q. Zhu, Metabolic footprinting of extracellular metabolites of brain endothelium infected with Neospora caninum in vitro, BMC Res. Notes 7 (2014) 406. https://doi.org/10.1186/1756-0500-7-406

[13] K.L. Liew, J.M. Jee, I. Yap, P.V.C. Yong, In vitro analysis of metabolites secreted during infection of lung epithelial cells by Cryptococcus neoformans, PLoS One 11(4) (2016) e0153356. https://doi.org/10.1371/journal.pone.0153356

[14] L. Casadei, M. Valerio, ^{1}H NMR metabolomic footprinting analysis for the in vitro screening of potential chemopreventive agents, in: S. Strano (Ed.), Cancer chemoprevention: Methods and protocols, Methods in molecular biology, vol. 1379, Human press, New York, 2016, pp 89-97. https://doi.org/10.1007/978-1-4939-3191-0_8

[15] A.R. Lima, A.M. Araujo, J. Pinto, C. Jeronimo, R. Henrique, M. de Lourdes Bastos, M. Carvalho, P. Guedes de Pinho, Discrimination between the human prostate normal and cancer cell exometabolome by GC-MS, Sci. Rep. 8 (2018) 5539. https://doi.org/10.1038/s41598-018-23847-9

[16] M.E. Knott, M. Manzi, N. Zabalegui, M.O. Salazar, L.I. Puricelli, M.E. Monge, Metabolic footprinting of a clear cell renal cell carcinoma in vitro model for human kidney cancer detection, J. Proteome Res. 17 (2018) 3877-3888. https://doi.org/10.1021/acs.jproteome.8b00538

[17] A. Seenivasan, J. Satya Eswari, P. Sankar, S.N. Gummadi, T. Panda, Ch. Venkateswarlu, Metabolic pathway analysis and dynamic macroscopic model development for lovastatin production by Monascus purpureus using metabolic footprinting concept, Biochem. Eng. J. 154 (2020) 107437. https://doi.org/10.1016/j.bej.2019.107437

[18] S.E. Mohmad-Saberi, Y.Z.H.Y. Hashim, M. Mel, A. Amid, R. Ahmad-Raus, V. Packeer-Mohamed, Metabolomics profiling of extracellular metabolites in CHO-K1 cells cultured in different types of growth media, Cytotechnology 65 (2013) 577-586. https://doi.org/10.1007/s10616-012-9508-4

[19] E. Dumont, C. De Bleye, P.-Y. Sacré, L. Netchacovitch, Ph. Hubert, E. Ziemons, From near-infrared and Raman to surface-enhanced Raman spectroscopy: Progress, limitations, perspectives in bioanalysis, Bioanalysis 8(10) (2016) 1077-1103. https://doi.org/10.4155/bio-2015-0030.

[20] C. Zong, M. Xu, L.-J. Xu, T. Wei, X. Ma, X.-S. Zheng, R. Hu, B. Ren, Surface-enhanced Raman spectroscopy for bioanalysis: Reliability and challenges, Chem. Rev. 118 (2018) 4946-4980. https://doi.org/10.1021/acs.chemrev.7b00668

[21] J. Cailletaud, C. De Bleye, E. Dumont, P.-Y. Sacré, L. Netchacovitch, Y. Gut, M. Boiret, Y.-M. Ginot, Ph. Hubert, E. Ziemons, Critical review of surface-enhanced Raman spectroscopy applications in the pharmaceutical field, J. Pharm. Biomed. Anal. 147 (2018) 458-472. https://doi.org/10.1016/j.jpba.2017.06.056

[22] M.S. Zalaffi, N. Karimian, P. Ugo, Review – Electrochemical and SERS sensors for cultural heritage diagnostics and conservation: Recent advances and prospects, J. Electrochem. Soc.167 (2020) 037548. https://doi.org/10.1149/1945-7111/ab67ac

[23] T.T.X. Ong, E.W. Blanch, O.A.H. Jones, Surface Enhanced Raman Spectroscopy in environmental analysis, monitoring and assessment, Sci. Total Environ. 720 (2020) 137601. https://doi.org/10.1016/j.scitotenv.2020.137601

[24] Z. Lin, L. He, Recent advance in SERS techniques for food safety and quality analysis: a brief review, Curr. Opin. Food Sci. 28 (2019) 82-87. https://doi.org/10.1016/j.cofs.2019.10.001

[25] M. Erzina, A. Trelin, O. Guselnikova, B. Dvorankova, K. Strnadova, A. Perminova, P. Ulbrich, D. Mares, V. Jerabek, R. Elashnikov, V. Svorcik, O. Lyutakov, Precise cancer detection via the combination of functionalized SERS surfaces and convolutional neural network with independent inputs, Sens. Actuators B Chem. 308 (2020) 127660. https://doi.org/10.1016/j.snb.2020.127660

[26] J. Plou, I. García, M. Charconnet, I. Astobiza, C. García- Astrain, C. Matricardi, A. Mihi, A. Carracedo, L.M. Liz- Marzán, Multiplex SERS detection of metabolic alterations in tumor extracellular media, Adv. Funct. Mater. 30 (2020) 1910335. https://doi.org/10.1002/adfm.201910335

[27] H. Cho, S. Kumar, D. Yang, S. Vaidyanathan, K. Woo, I. Garcia, H.J. Shue, Y. Yoon, K. Ferreri, H. Choo, Surface-enhanced Raman spectroscopy-based label-free insulin detection at physiological concentrations for analysis of islet performance, ACS Sens. 3(1) (2018) 65-71. https://doi.org/10.1021/acssensors.7b00864

[28] D. Li, L. Jiang, J.A. Piper, I.S. Maksymov, A.D. Greentree, E. Wang, Y. Wang, Sensitive and multiplexed SERS nanotags for the detection of cytokines secreted by lymphoma, ACS Sens. 4 (2019) 2507-2514. https://doi.org/10.1021/acssensors.9b01211

[29] F. Lussier, D. Missirlis, J.P. Spatz, J.-F. Masson, Machine-learning-driven surface-enhanced Raman scattering optophysiology reveals multiplexed metabolite gradients near cells, ACS Nano 13(2) (2019) 1403-1411. https://doi.org/10.1021/acsnano.8b07024

[30] N. Liu, M. Tang, J. Ding, The interaction between nanoparticles-protein corona complex and cells and its toxic effect on cells, Chemosphere 245 (2020) 125624. https://doi.org/10.1016/j.chemosphere.2019.125624

[31] E. Dumont, C. De Bleye, J. Cailletaud, P.-Y. Sacré, P.-B. Van Lerberghe, B. Rogister, G.A. Rance, J.W. Aylott, Ph. Hubert, E. Ziemons, Development of a SERS strategy to overcome the nanoparticle stabilisation effect in serum-containing samples: Application to the quantification of dopamine in the culture medium of PC-12 cells, Talanta 186 (2018) 8-16. https://doi.org/10.1016/j.talanta.2018.04.038

[32] J. Kneipp, H. Kneipp, M. McLaughlin, D. Brown, K. Kneipp, In vivo molecular probing of cellular compartments with gold nanoparticles and nanoaggregates, Nano Lett. 6 (2006) 2225-2231. https://doi.org/10.1021/nl061517x

[33] V. Moisoiu, A. Stefancu, D. Gulei, R. Boitor, L. Magdo, L. Raduly, S. Pasca, P. Kubelac, N. Mehterov, V. Chiș, M. Simon, M. Muresan, A.I. Irimie, M. Baciut, R. Stiufiuc, I.E. Pavel, P. Achimas-Cadariu, C. Ionescu, V. Lazar, V. Sarafian, I. Notingher, N. Leopold, I. Berindan-Neagoe, SERS-based differential diagnosis between multiple solid malignancies: breast, colorectal, lung, ovarian and oral cancer, Int. J. Nanomedicine 14 (2019) 6165-6178. https://doi.org/10.2147/IJN.S198684

[34] H. Torul, H. Çiftçi, D. Çetin, Z. Suludere, I.H. Boyacı, U. Tamer, Paper membrane-based SERS platform for the determination of glucose in blood samples, Anal. Bioanal. Chem. 407 (2015) 8243-8251. https://doi.org/10.1007/s00216-015-8966-x

[35] N.E. Markina, A.V. Markin, K. Weber, J. Popp, D. Cialla-May, Liquid-liquid extraction-assisted SERS-based determination of sulfamethoxazole in spiked human urine, Anal. CHim. Acta 1109 (2020) 61-68. https://doi.org/10.1016/j.aca.2020.02.067

[36] H. Chon, R. Wang, S. Lee, S.-Y. Bang, H.-S. Lee, S.-C. Bae, S.H. Hong, Y.H. Yoon, D.W. Lim, A.J. deMello, J. Choo, Clinical validation of surface-enhanced Raman scattering-based immunoassays in the early diagnosis of rheumatoid arthritis, Anal. Bioanal. Chem. 407 (2015) 8353-8362. https://doi.org/10.1007/s00216-015-9020-8

[37] M. Bhamidipati, G. Lee, I. Kim, L. Fabris, SERS-based quantification of PSMA in tissue microarrays allows effective stratification of patients with prostate cancer, ACS Omega 3 (2018) 16784-16794. https://doi.org/10.1021/acsomega.8b01839

[38] R. Xing, Y. Wen, Y. Dong, Y. Wang, Q. Zhang, Z. Liu, Dual molecularly imprinted polymer-based plasmonic immunosandwich assay for the specific and sensitive detection of protein biomarkers, Anal. Chem. 91 (2019) 9993-10000. https://doi.org/10.1021/acs.analchem.9b01826

[39] Z. Ye, C. Li, Q. Chen, Y. Xu, S.E.J. Bell, Ultra- stable plasmonic colloidal aggregates for accurate and reproducible quantitative SE(R)RS in protein- rich biomedia, Angew. Chem. Int. Ed. 58 (2019) 19054-19059. https://doi.org/10.1002/anie.201911608

[40] V. Shalabaeva, L. Lovato, R. La Rocca, G.C. Messina, M. Dipalo, E. Miele, M. Perrone, F. Gentile, F. De Angelis, Time resolved and label free monitoring of extracellular metabolites by surface enhanced Raman spectroscopy, PLos ONE 12(4) (2017) e0175581. https://doi.org/10.1371/journal.pone.0175581

[41] M. Hassoun, J. Rüger, T. Kirchberger-Tolstik, I.W. Schie, T. Henkel, K. Weber, D. Cialla-May, C. Krafft, J. Popp, A droplet-based microfluidic chip as a platform for leukemia cell lysate identification using surface-enhanced Raman scattering, Anal. Bioanal. Chem. 410 (2018) 999-1006. https://doi.org/10.1007/s00216-017-0609-y

[42] W. Li, X. Zhao, Z. Yi, A.M. Glushenkov, L. Kong, Plasmonic substrates for surface enhanced Raman scattering, Anal. Chim. Acta 984 (2017) 19-41. https://doi.org/10.1016/j.aca.2017.06.002

[43] E. Le Ru, P. Etchegoin, Metallic colloids and other SERS substrates, in: E. Le Ru, P. Etchegoin (Eds), Principles of Surface-enhanced Raman spectroscopy and related plasmonic effects, Elsevier, Amsterdam, 2009, pp 367-413. https://doi.org/10.1016/B978-0-444-52779-0.00013-1

[44] R. Shi, X. Liu, Y. Ying, Facing challenges in real-life application of surface-enhanced Raman scattering: Design and nanofabrication of surface-enhanced Raman scattering substrates for rapid field test of food contaminants, J. Agric. Food Chem. 66 (2018) 6525-6543. https://doi.org/10.1021/acs.jafc.7b03075

[45] E. Dumont, C. De Bleye, M. Haouchine, L. Coïc, P.-Y. Sacré, Ph. Hubert, E. Ziemons, Effect of the functionalisation agent on the surface-enhanced Raman scattering (SERS) spectrum: Case study of pyridine derivatives, Spectrochim. Acta A Mol. Biomol. Spectrosc. 233 (2020) 118180. https://doi.org/10.1016/j.saa.2020.118180

[46] L.M. Sherman, A.P. Petrov, L.F.P. Karger, M.G. Tetrick, N.J. Dovichi, J.P. Camden, A surface-enhanced Raman spectroscopy database of 63 metabolites, Talanta 210 (2020) 120645. https://doi.org/10.1016/j.talanta.2019.120645

[47] P.C. Lee, D. Meisel, Adsorption and surface-enhanced Raman of dyes on silver and gold sols, J. Phys. Chem. 86 (1982) 3391-3395. https://doi.org/10.1021/j100214a025

[48] H. Wu, T.H. Denna, J.N. Storkersen, V.A. Gerriets, Beyond a neurotransmitter: The role of serotonin in inflammation and immunity, Pharmacol. Res. 140 (2019) 100-114. https://doi.org/10.1016/j.phrs.2018.06.015

[49] B. Olivier, Serotonin: A never-ending story, Eur. J. Pharmacol. 753 (2015) 2-18. https://doi.org/10.1016/j.ejphar.2014.10.031

[50] E. Vander Ende, M.R. Bourgeois, A.-I. Henry, J.L. Chávez, R. Krabacher, G.C. Schatz, R.P. Van Duyne, Physicochemical trapping of neurotransmitters in polymer-mediated gold

nanoparticle aggregates for surface-enhanced Raman spectroscopy, Anal. Chem. 91 (2019) 9554-9562. https://doi.org/10.1021/acs.analchem.9b00773

[51] G. Rademaker, B. Costanza, S. Anania, F. Agirman, N. Maloujahmoum, E. Di Valentin, J.- J. Goval, A. Bellahcène, V. Castronovo, O. Peulen, Myoferlin contributes to the metastatic phenotype of pancreatic cancer cells by enhancing their migratory capacity through the control of oxidative phosphorylation, Cancer 11 (2019) 853. https://doi.org/10.3390/cancers11060853

[52] S.E.J. Bell, G. Charron, E. Cortés, J. Kneipp, M. Lamy de la Chapelle, J. Langer, M. Prochazka, V. Tran, S. Schlücker, Towards reliable and quantitative surface-enhanced Raman scattering (SERS): From key parameters to good analytical practice, Angew. Chem. Int. Ed. 59 (2020) 2-11. https://doi.org/10.1002/anie.201908154

[53] E. López-Tobar, B. Hernández, A. Chenal, Y.-M. Coïc, J. Gómez Santos, E. Mejía-Ospino, J.V. Garcia-Ramos, M. Ghomi, S. Sanchez-Cortes, Large size citrate-reduced gold colloids appear as optimal SERS substrates for cationic peptides, J. Raman Spectrosc. 48 (2017) 30-37. https://doi.org/10.1002/jrs.4976

[54] R. García-Alvarez, M. Hadjidemetriou, A. Sánchez-Iglesias, L.M. Liz-Marzan, K. Kostarelos, In vivo formation of protein corona on gold nanoparticles. The effect of their size and shape, Nanoscale 10 (2018) 1256-1264. https://doi.org/10.1039/C7NR08322J

[55] M. Krzan, H. Caps, N. Vandewalle, High stability of the bovine serum albumine foams evidenced in Hele-Shaw cell, Colloids Surf. A Physicochem. Eng. Asp. 438 (2013) 112-118. https://doi.org/10.1016/j.colsurfa.2013.01.012

Figure captions

Figure 1: Description of the protein removal device, used in a non-invasive manner (a) or in an invasive one (b).

Figure 2: SERS spectra obtained by analysing a 50/50 (v/v) mixture of AuNPs with either pure RPMI, the RPMI used as collection medium under the insert or the culture medium (CM) inside the insert. Pictures of mixtures of these media with AuNPs are displayed on the right to highlight the (absence of) AuNPs aggregation.

Figure 3: SERS spectra collected during 24 h with the TruScan™ using the non-invasive approach (a) or by analysing samples of the collection medium collected in an invasive way (c). The asterisks highlight the specific bands of 2-MP. The 2 intense bands located at 1003 and 1033 cm^{-1} in a) are due to polystyrene, coming from the bottom of the multi-well plate. Evolution of the area of the 1083 cm^{-1} band over time (b,d). Differences in the Raman intensity scale between a) and c) can be explained by different detector signal processing by the two Raman spectrophotometers.

Figure 4: Plot of the first 2 PCs of the PCA (3 PCs) obtained for the 5-HT diffusion data (a). Comparison of PC2 with a reference 0.1 ppm 5-HT spectrum obtained with AuNPs in suspension (b). Characteristic bands of 5-HT are evidenced by asterisks.

Figure 5: Plot of the first 2 PCs of the PCA (3 PCs) obtained for the 5-HT diffusion data in the melted plate (a). Comparison of the inverse of PC1 with a reference 0.1 ppm 5-HT spectrum obtained with AuNPs in suspension (b). Characteristic bands of 5-HT are evidenced by asterisks.

Figure 6: PC1/PC2 (a) and PC1/PC3 (b) plot of the PCA (4 PCs) applied on all conditioned media diffusion data. Asterisks represent pure culture medium (CM) data, whereas dots and stars depict high and low metastatic cell conditioned media data (HM and LM), respectively. The blue-to-yellow shading shows the effect of diffusion time. The red circles indicate data related to the spectra acquired during the first day, and the black arrows in a) point a time-related trend out.

Figure 7: Comparison of the mean SERS spectra of pure culture medium (CM), high and low metastatic cell conditioned media (HM and LM, respectively) acquired after 48h of diffusion with

the TruScan™. The asterisks flag spectral regions that are not linked to the Au-coverslip and that can thus be used to differentiate the 3 kinds of sample.

Figure 8: PC1/PC2 plots of the PCA (a) and d): 3 PCs; b) and c): 2 PCs included in the PCA models) realised on the mean spectra acquired through the bottom of the multi-well plate at several cell incubation times (16h, 24h15, 48h15 and 67h35). Orange and purple circles surround low metastatic (LM) and high metastatic (HM) cell samples, respectively. Orange arrows indicate trends related to LM cell densities, while purple ones highlight trends related to HM cell densities (pointing from the lowest to the highest cell densities).

Figure 1

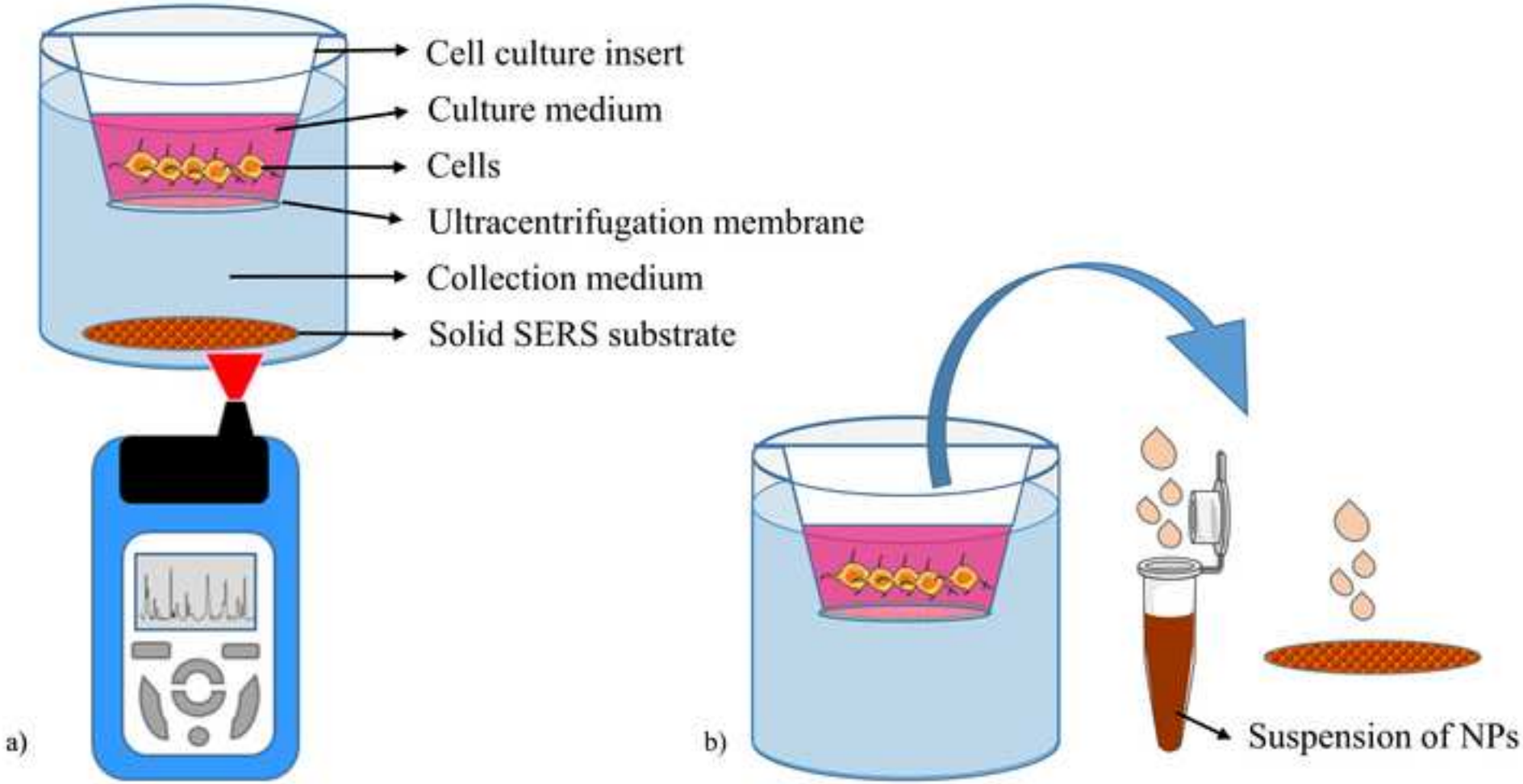

Figure 2

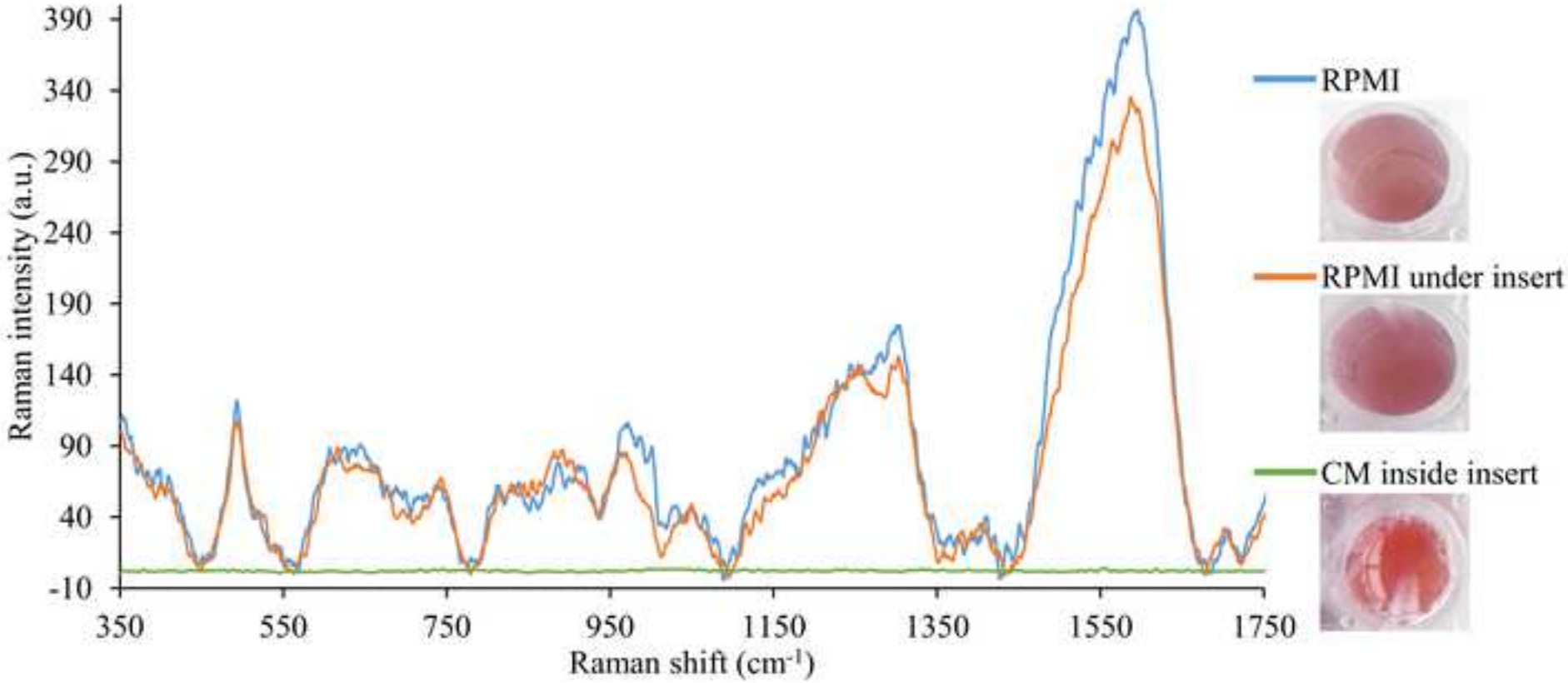

Figure 3

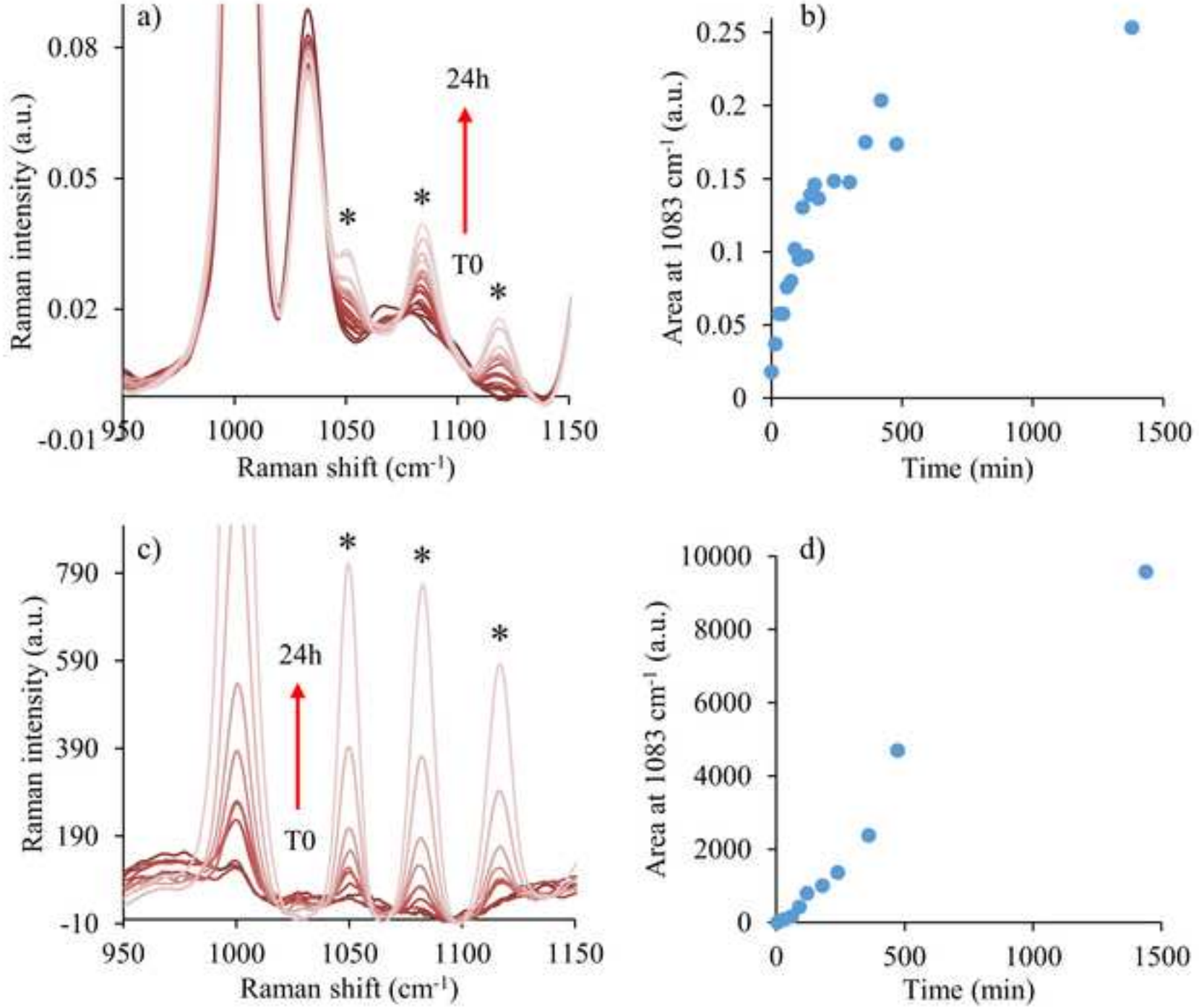

Figure 4

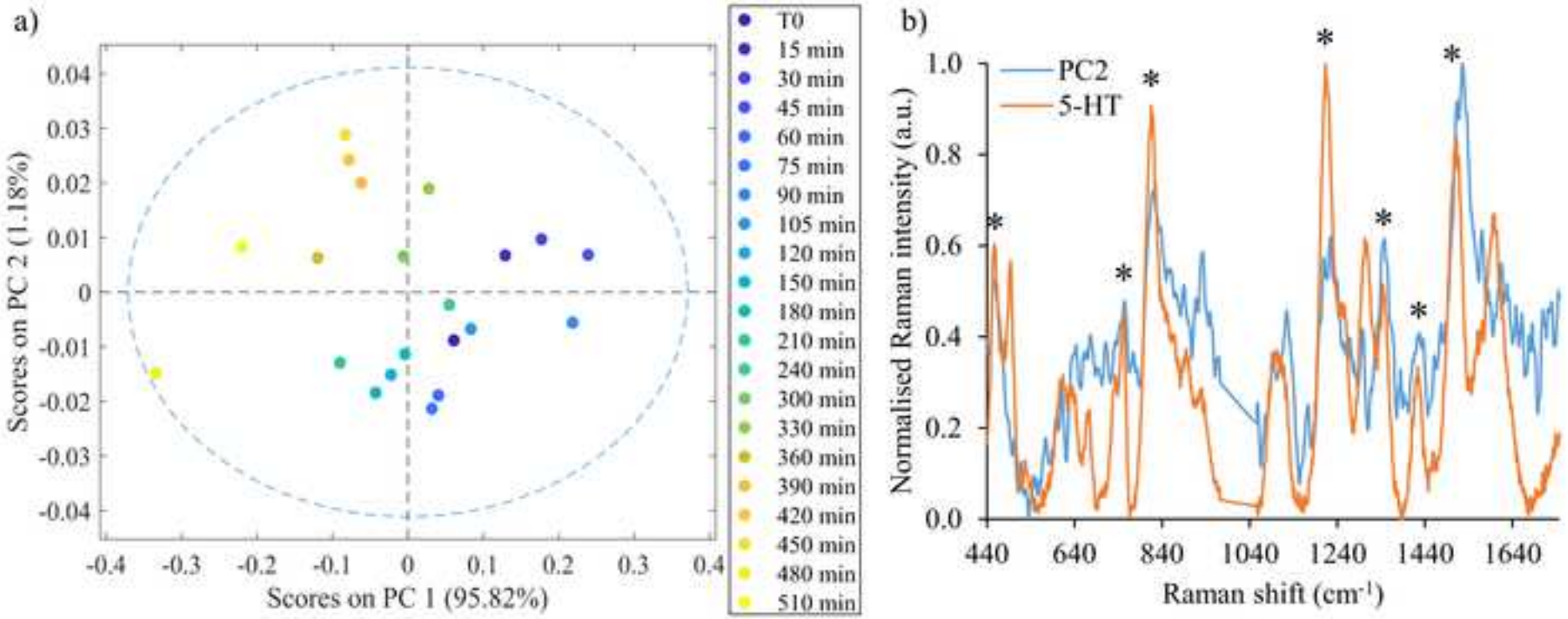

Figure 5

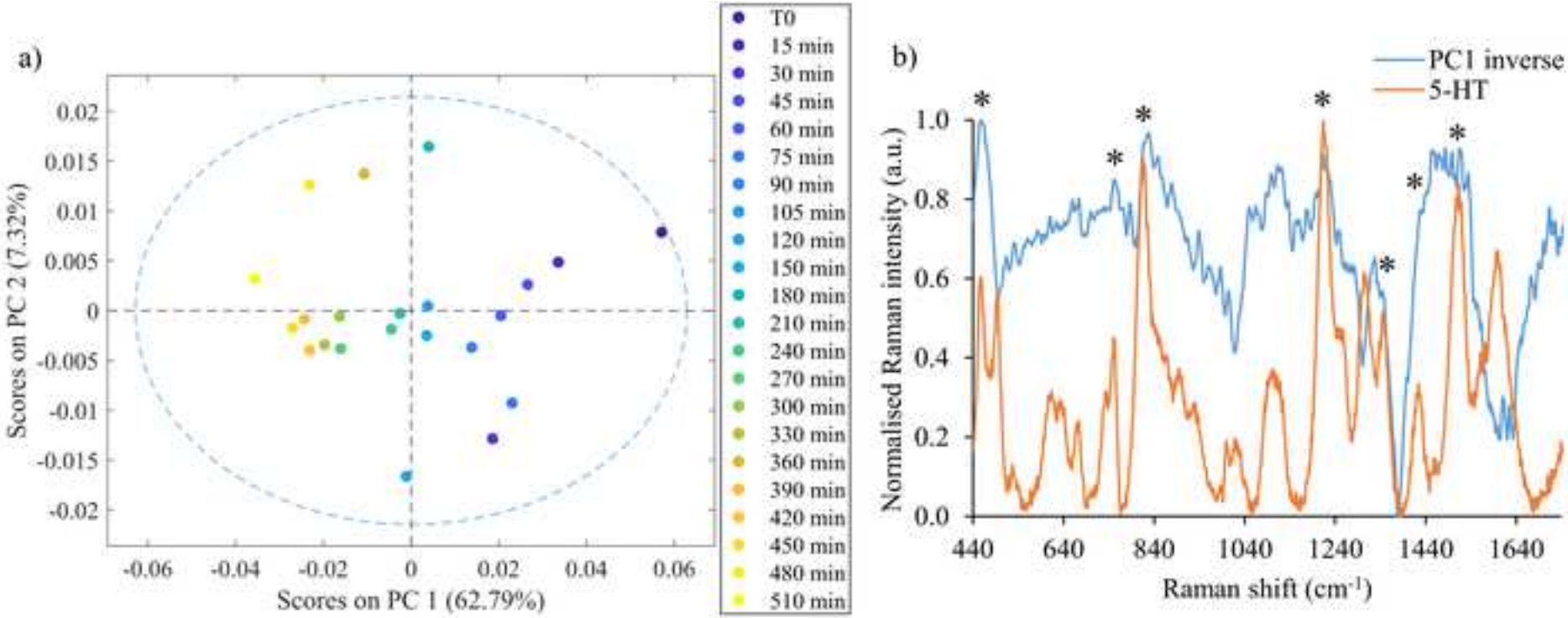

Figure 6

Click here to access/download;Figure;Figure 6.tif

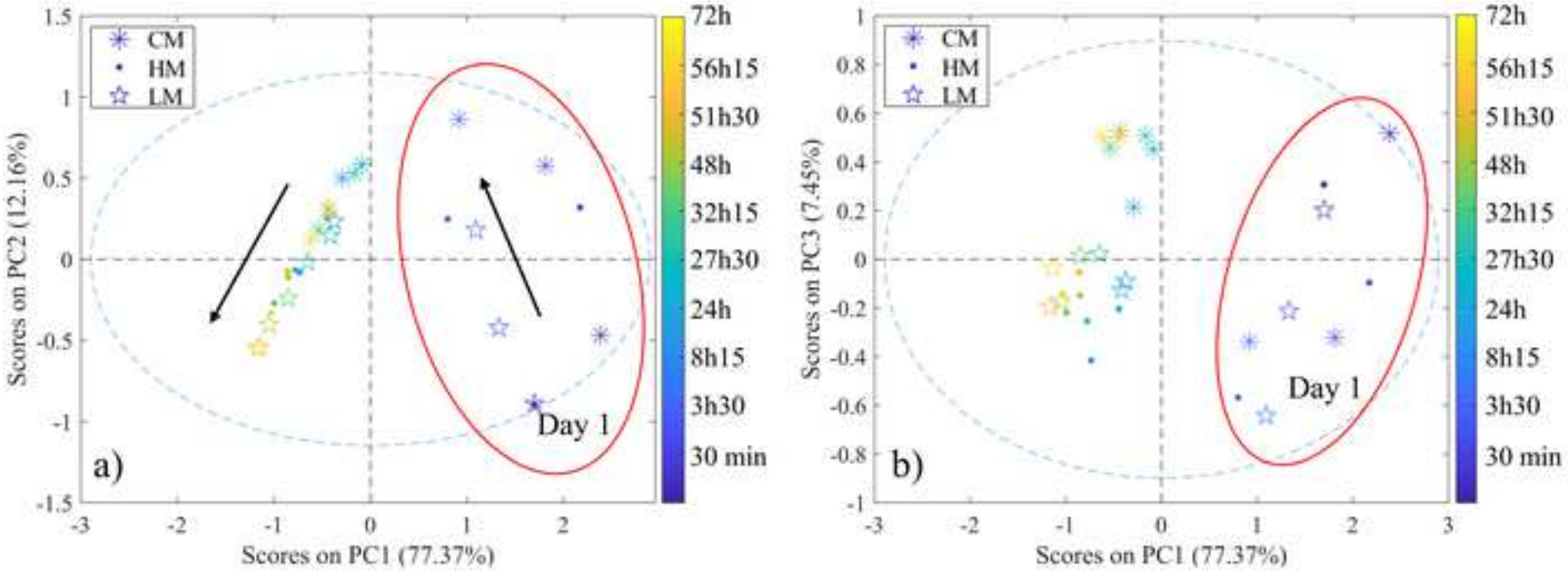

Figure 7

Click here to access/download;Figure;Figure 7.tif

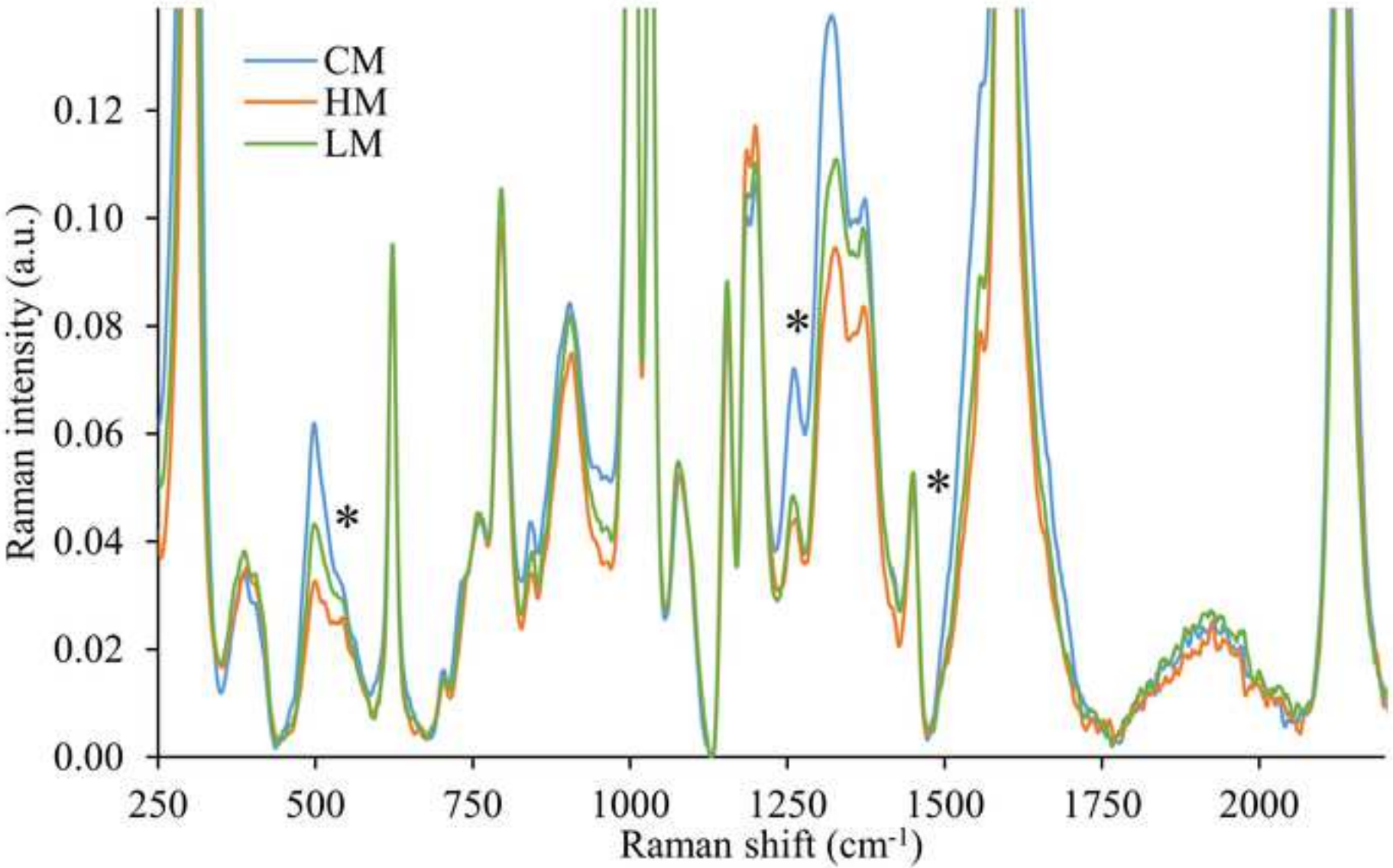

Figure 8

Click here to access/download;Figure;Figure 8.tif